

MB ROHWER*, MK MATHE, S HIETKAMP, RM MODIBEDI, PT NONJOLA, T MASOMBUKA
*CSIR Materials Science and Manufacturing, Energy and Processes, PO Box 395, Pretoria, 0001
Email: mrohwer@csir.co.za

Abstract

Fuel cells can contribute to energy security, because they possess the potential to convert potentially renewable fuels such as hydrogen, methanol or ethanol cleanly and efficiently into electrical energy. They are of particular interest to South Africa, as they incorporate catalytic metals, e.g. Platinum, of which three-quarters of known reserves are found in South Africa.

The authors' work hitherto was focused on developing, evaluating and improving the key electrochemical components of fuel cells, i.e. membranes, catalysts, gas diffusion layers and electrodes. This paper highlights the results achieved to date in the fields of hydrogen fuel cells, direct alcohol fuel cells and anionic membranes.

Furthermore, the paper describes how a test cell design from Helsinki University of Technology was modified to improve the geometric utilisation of the flow field plates, to allow upgrading from a single cell to a stack, as well as to measure and control temperature.

1. Introduction

A fuel cell is a device that converts the chemical energy of a fuel directly to electrical energy. In this respect, it is similar to a battery. However, the chemical energy for a fuel cell is not necessarily stored inside the cell. Rather, it can be supplied externally, and the fuel cell can continue to operate as long as it is supplied with fuel.

A fuel cell has two compartments: in the anode, fuel (e.g. hydrogen gas) is oxidised, while in the cathode, oxygen (either pure or in the form of air) is reduced. In the process, the fuel cell delivers an electrical current to an external circuit.

While fuel cells can generate electricity directly from fuel, conventional production of electricity from fossil fuels involves a step-wise conversion of the chemical energy in the fuel - first to thermal energy, then to kinetic energy and only then to electrical energy. Each of these steps involves

losses. Fuel cells, being direct energy converters, therefore have much potential as highly efficient energy sources, provided that they can be operated at high efficiency.

A number of aspects must still be optimised in order to make fuel cells truly efficient and cost-effective energy converters. They include amongst others, catalysis (Litster and McLean, 2004; Watanabe, 2003), mass transport (Chen *et al.*, 2008; Song *et al.*, 2001), ionic and electric conductivity (Zawodzinski *et al.*, 1993) and water management (Yousfi-Steiner *et al.*, 2008).

This paper describes our research activities in some of these fields, specifically the following:

- 1) Reducing the cost and improving the performance of hydrogen fuel cells by optimising the loading of catalyst (being expensive noble metals) and ionomer;
- 2) Improving conventional acidic direct alcohol fuel cells by developing more efficient catalysts and by investigating other fuels than methanol;
- 3) Investigating anionic membranes for use in alkaline direct alcohol fuel cells, as cheaper and more efficient alternatives to conventional acidic direct alcohol fuel cells.

The aim of the authors' research activities is to develop fuel cell components and products with new and improved features.

2. Research Activities

2.1 Hydrogen fuel cells

2.1.1 Background

Hydrogen-fuelled Polymer Electrolyte Membrane Fuel Cells (PEMFC) are the most widely researched and developed type of fuel cell, and some systems have already been commercialised. Hence, they served as a suitable starting point for our research. They typically utilise Nafion® as membrane material and Pt as catalyst, and one of the drawbacks is that both these components add significantly to the overall cost of a PEMFC.

We focused our research activities on:

- 1) The effect of the loading of catalytic ink on cell performance;
- 2) The effect of the ionomer content in the catalytic ink;
- 3) Testing the reproducibility of the Membrane Electrode Assembly (MEA) fabrication technique.

The function of the ionomer (Nafion solution) in the MEA is to conduct protons in the catalytic layer (Qi and Kaufman, 2002; Wilson *et al.*, 1995). However, there is a limit to the amount that can be added, since the other properties of the ionomer film, such as low gas permeability and poor electric conductivity, might affect the cell performance unfavourably (Reiner *et al.*, 2006).

2.1.2 Experimental

Catalytic ink was prepared by dispersing a specific amount of 20% Pt/C in de-ionised water followed by addition of isopropanol and 5 wt% Nafion solution. The mixture was stirred magnetically, followed by sonication in order to disperse the particles. The amount of Nafion solution added to the catalytic ink was varied from 0 to 58% (measured as dry ionomer mass with respect to the mass of Pt/C). The homogeneous suspension was sonicated until the desired viscosity was obtained. Gas diffusion layers (carbon cloth type A- 0.35mm in thickness, used as received from PEMEAS) were cut out and weighed. The resulting ink was air-sprayed over the carbon cloths, varying the catalyst loading at 0.15, 0.1 and 0.05 mg Pt/cm². The catalytic carbon cloths were then allowed to air-dry and heated at 80°C for 30 min. The mass of the catalytic carbon cloths was recorded. Nafion® 112 membrane (51µm, Du Pont Inc.) was boiled in 3 wt.% H₂O₂ solution for an hour and rinsed in boiling de-ionised water for 1 hr. In order to remove metallic contaminants on the membrane surface and to obtain a proton exchange form of membrane, it was boiled in 0.5 M H₂SO₄ for 1 hr. Finally, it was rinsed again in boiling de-ionised water for 1 hr. The MEA was prepared by sandwiching the pretreated Nafion 112 between two catalytic carbon cloths and hot pressing at 110°C for 3 min. The MEAs made in-house, were tested in a commercial PEMFC (supplied by Heliocentris Energiesysteme GmbH, 7.5cm² active surface area, assembled at 77cNm). Hydrogen and oxygen were fed respectively to the anode and

cathode, after passing through bubbler humidifiers at room temperature.

2.1.3 Key findings

MEAs of varying Pt loadings and ionomer content were successfully prepared using the air-spray method. The performance of the cell increased with an increase in Pt loading. 41wt.% ionomer (relative to Pt/C mass) was found to be the optimum ionomer percentage. This is similar to literature (Passalacqua *et al.*, 1998; Lee *et al.*, 1998; Passalacqua *et al.*, 2001), where the optimal ionomer percentage is ca. 30% at Pt loadings of 0.1 to 0.4 mg/cm². The results are summarized in figure 1.

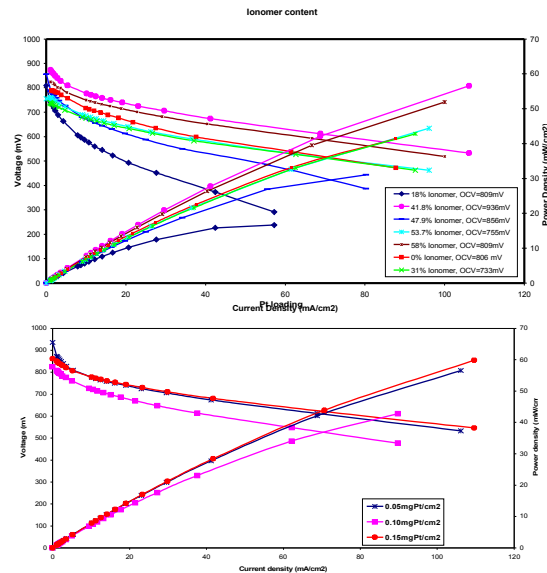


Figure 1: Performance curves illustrating the effect of ionomer content at 0.05mgPt/cm² and Pt loading for 41.8wt% ionomer in the catalytic layer respectively.

Increasing the ionomer loading above 0.23, 0.37 and 0.54mg/cm² for 0.05, 0.10 and 0.15 mg Pt/cm² respectively, did not improve cell performance significantly. The maximum power densities obtained with these loadings at room temperature were 51, 59 and 69 mW/cm² respectively, compared to 306 mW/cm² achieved in literature (Passalacqua *et al.*, 1998) at 70°C.

The air-spray method was found to be reproducible for all ionomer and Pt loadings studied, since the

performance curves of the MEAs did not show a significant difference.

2.2 Direct alcohol fuel cells

2.2.1 Background

Direct alcohol fuel cells use an alcohol, mostly methanol, as fuel. The direct methanol fuel cell (DMFC) is a very promising power source for portable devices (e.g. laptops and cellular phones) and is suitable for remote locations.

The methanol oxidation process has parallel reaction pathways requiring a catalyst capable of breaking the C-H bond and facilitating the reaction of the resulting residue with oxygen to form CO₂. Platinum is recognised to be the most active metal for methanol oxidation; however, CO is formed as an intermediate and adsorbs strongly to the Pt surface, blocking it for further methanol adsorption. This leads to very low power densities (Burstein *et al.*, 1997). Pt-Ru is the most promising binary catalyst for methanol oxidation due to its improved CO tolerance. On the other hand, the power density of Pt-Ru anode catalyst for DMFC is about a factor of 10 lower than that of the hydrogen PEMFC (Watanabe *et al.*, 1987; Lee *et al.*, 2006; Xing *et al.*, 2006). Hence, it is important to investigate other ways of improving Pt-Ru performance and other catalysts that will oxidise methanol. In this paper Pt-Ru/C is prepared using a chemical impregnation method in order to determine the effect of the reducing agent (formic acid and sodium hypophosphite) on Pt-Ru/C properties for methanol electro-oxidation.

2.2.2 DMFC catalysts

2.2.2.1 Preparation of catalysts

2M formic acid (Sigma-Aldrich) was added to carbon black (Vulcan XC-72, Cabot Corporation) and heated to 80°C while stirring for 20 min. to make a suspension. Aqueous solutions of H₂PtCl₆·6H₂O (Sigma-Aldrich) and RuCl₃·xH₂O (Sigma-Aldrich) (Pt:Ru molar ratios of 1:1) were slowly added to the Vulcan XC-72 suspension with stirring to make a slurry. The slurry was left to cool at room temperature, then filtered and washed with de-ionised water to remove chloride ions. The catalyst was allowed to air-dry and further dried at 80°C for 1 hour. This catalyst is denoted as Pt-

Ru/C (FAM). The second catalyst was prepared using sodium hypophosphite (NaH₂PO₂·H₂O purchased from Sigma Aldrich) as the reducing agent, following the preparation method of Xing *et al.* (Xing *et al.*, 2006). This catalyst is denoted as Pt-Ru/C (SPM).

2.2.2.2 Characterisation of catalysts

XRD patterns were examined using a Phillips PW 1830 X-ray diffractometer generator operating at 45 kV and 40 mA. Copper K-α1 radiation source with a wavelength of 1.5406 Å. The samples were run from 5° to 90° 2θ, step size of 0.02° 2θ and step time 2 seconds or 1 second. LEO 1525 Field Emission Scanning Electron Microscope with INCA software by Oxford for Energy Dispersive X-ray Spectroscopy was used to estimate the elemental composition of different regions of the catalysts. Methanol oxidation activity was determined using cyclic voltammetry and linear chronoamperometry in a three-electrode cell, using an AutoLab Potentiostat/Galvanostat/FRA at room temperature. A Pt rod and Ag/AgCl (3M KCl) were used respectively as counter and reference electrodes. The cell was purged with nitrogen gas (99.99%) for 60 min. before the experiments. 0.05g of the electrocatalyst powder, 5ml de-ionised water and 1ml 5wt% Nafion solution (Du-Pont) were ultrasonicated for 20 min. to prepare a catalytic ink. 1µl of the ink was pipetted onto a polished glassy carbon disk electrode with area of 0.071 cm², air-dried for 30 min. and then at 90°C for 15 min.

2.2.2.3 Key findings

In cyclic voltammetry, onset potential of methanol oxidation in a positive scan is a key factor for evaluating the catalyst activity. Table 1 shows the onset potentials and the platinum crystal sizes obtained respectively from cyclic voltammograms and XRD.

Table 1: Onset potential and the crystal size of prepared electro-catalysts

Electro-catalyst	Onset Potential (V vs. Ag/AgCl) 0.5M H ₂ SO ₄ + 0.5M MeOH	Pt Crystal size (nm)
Pt-Ru/C ETEK	0.15	-
Pt-Ru/C (FAM)	0.18	3.6
Pt-Ru/C (SPM)	0.16	3.3
Pt-Ir/C (FAM)	0.23	3.7

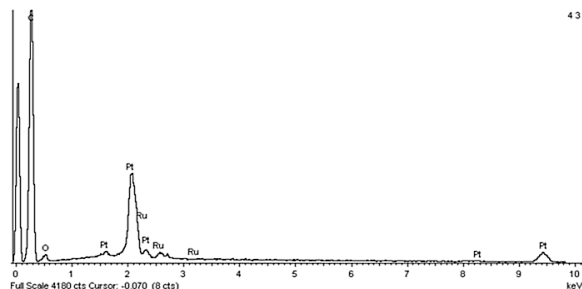
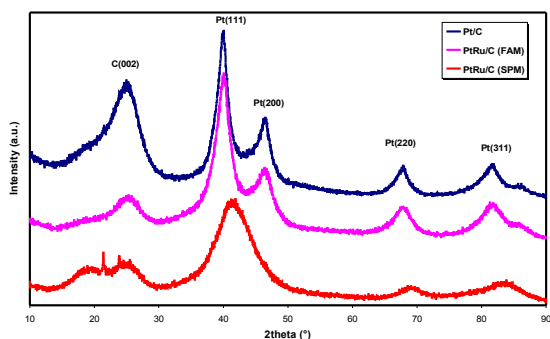


Figure 2: XRD and EDX profiles of in-house catalysts

The lower the onset potential, the more active the catalyst is towards methanol oxidation. According to the table above, commercial Pt-Ru/C ETEK has a lower onset potential than in-house prepared catalysts. Research in producing electrocatalysts with onset potential lower than 0.15V is ongoing; one of the approaches is the use of carbon nanotubes as a support material for the Pt-Ru/C (SPM). The prepared catalysts will be used as the anode of an MEA and then tested for performance in a DMFC.

2.2.3 Other alcohols as fuels for a PEM DMFC

The fuel most widely used in direct alcohol fuel cells is methanol. However, the relative toxicity of methanol, both acute and chronic (ACGIH, 1991), makes it less attractive as a fuel than other alcohols, e.g. ethanol, ethylene glycol or glycerol. The use of various alcohols in a direct alcohol fuel cell with an alkaline membrane has been reported in literature (Ogumi *et al.*, 2005). The authors used a poly-olefin based, quaternised AEM similar to those described in section 2.3 of this paper, and ranked the alcohols in terms of reactivity (i.e. power output from the cell) as follows: ethylene glycol > glycerol > methanol > erythritol > xylitol.

We conducted a similar study, using a commercial PEM DMFC to evaluate the performance of methanol, ethanol, isopropanol, ethylene glycol and glycerol. The cell was supplied by Heliocentris Energiesysteme GmbH and uses Pt-Ru/C as anode catalyst and Pt/C as cathode catalyst.

All five alcohols were diluted in de-ionised water to a concentration of 1.5 M. The open cell voltage was measured, after which the cell was connected to a 10 Ohm load and the voltage and current measured. Using these values and the active surface area of the cell (7.5 cm²), the power density was calculated for each alcohol.

2.2.3.1. Key findings

The MEA used in the cell had not been used for a prolonged period, resulting in a dehydrated polymer electrolyte. This was evident from very poor performance (in the order of 0.1 mW / cm²) during initial runs. The runs were repeated with the different fuels until repeatable results were achieved for each alcohol, presented in table 2.

Table 2: Power densities achievable with various alcohols in a commercial DMFC

Alcohol	Power density (mW / cm ²)
Methanol	0.908
Ethanol	0.894
Isopropanol	4.152
Ethylene glycol	0.616
Glycerol	0.517

The reactivity series can therefore be expressed as follows:

Isopropanol >> Methanol ~ Ethanol > Ethylene glycol > Glycerol

Isopropanol is the obvious out-lier amongst these results. While filling and emptying the cell, it was observed that isopropanol exhibited the best wetting (dispersant / surfactant) properties of all the alcohols used. We surmise that the wetting effect promoted good mass transport through the gas diffusion layer (GDL), leading to improved performance. This will be the subject of further investigations.

Ethylene glycol is a diol, i.e. a 1.5 M solution contains 3.0 M of OH groups. Similarly, a solution of glycerol (a triol) at 1.5 M concentration contains 4.5 M of OH groups. Yet in spite of being poly-ols, both these alcohols exhibited lower performance in the PEM DMFC than the three mono-ols. This is in contrast to the previously mentioned oxidation of these poly-ols in an alkaline fuel cell, which gave higher performance than methanol. A satisfactory explanation still has to be found for this phenomenon.

Effervescence was observed on the anode GDL only when powering the cell with methanol. This indicates that the oxidation reaction proceeds fully only in the case of methanol, yielding CO₂ gas. The other fuels are presumably oxidised only partially.

2.3 Anionic membranes

2.3.1 Background

Proton conductive polymers such as Nafion® and Flemion® (perfluorinated polymers) are state-of-the-art materials and have been extensively

studied especially in fuel cell applications (Mauritz and Moore, 2004; Savadogo, 1998). When Nafion membranes (proton exchange membranes) are used in direct alcohol fuel cells (DAFCs), several major obstacles emerge, among them methanol crossover and relatively low activity (Savadogo, 2004). The crossover reduces the operational voltage and the power that can be achieved (Kim *et al.*, 2007). A further disadvantage of PEM-based fuel cells is the high cost of the MEA, related to:

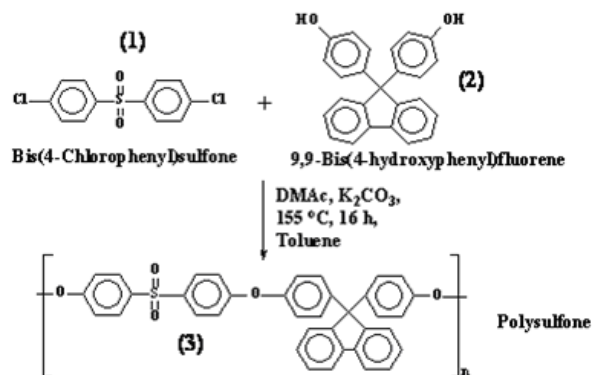
(i) an expensive polymeric membrane and
(ii) the use of platinum catalysts (Savadogo, 2004). A possible solution for these problems lies in the development of alternatives such as anionic exchange membranes (AEMs), which exhibit high conductivity and reduced alcohol permeation. Recent advances have allowed the production of membrane materials and ionomers that could facilitate the development of an alkaline equivalent to proton exchange membranes (PEMs). The application of these alkaline anion-exchange membranes (AAEMs) in fuel cells is a promising area for research. The advantages, disadvantages and the rationale behind alkaline fuel cells have been explained in detail in a literature review (Varcoe and Slade, 2005). One of the advantages is that in alkaline fuel cells, the pathway of the charge carrier (OH⁻) through the membrane is opposite to that of protons in the acidic PEM system. Hence, it opposes the direction of methanol flux through the membrane, leading to an intrinsic reduction of performance losses (Fang and Shen, 2006).

Our current research interest in this field concerns the development and characterisation of anion-exchange membranes from arylene ether sulfone polymers. As a class of high-performance engineering thermo-plastic materials, poly(arylene ethers) (PAEs) have a high glass transition temperature, high thermal stabilities, good mechanical properties and excellent resistance to hydrolysis and oxidation (McGrath *et al.*, 2002). Functionalised PAEs may find many applications as membrane materials for gas separation, water desalination, and in fuel cells.

2.3.2 Experimental

Initially, a poly(arylene ether) (PAE) was synthesised and characterised, to serve as a base polymer for an anion-exchange membrane (AEM). The PEA synthesis involved nucleophilic

displacement of activated aromatic halides in polar solvents by Friedel-Crafts process (Scheme 1) (Hergenrother *et al.*, 1988). In addition, two commercially available PAEs were sourced.



Scheme 1: Synthesis of compound (3)

Subsequently, all three PAE base polymers were converted into AEMs. While cation exchange membranes are typically prepared by aromatic sulfonation of a base polymer with sulfuric acid or the acid chloride, the AEMs were prepared from the aforementioned base polymers in two steps: firstly, by introducing chloromethyl groups as substituents in the presence of a Friedel-Crafts catalyst to an aromatic ring of the polymer (this was achieved by treating the polymer with chloromethyl octyl ether, synthesised separately), and secondly, by introducing quaternary ammonium groups into the chloromethylated polysulfone polymers (CMPSf) through treatment with trimethylamine.

All the AEM structures were determined by proton nuclear magnetic resonance spectroscopy ($^1\text{H-NMR}$) and/or Fourier-transform infrared spectroscopy (FT-IR). Thermogravimetric analysis (TGA) was used to determine the membranes' thermal stability and the fraction of volatile components by monitoring the weight change that occurred as the compounds were heated.

The structure of compound (3) was confirmed by $^1\text{H-NMR}$ spectroscopy, as shown in Figure 3. The integration of the multiplets are due to the aromatic hydrogen atoms, which showed two sets of doublet-doublet peaks (1,2,3, and 4), respectively ascribed to oxy-1,4-phenylenesulfone and oxy-1,4-phenylenecarbon at $\sim d_{\text{H}}$ 6.85, 6.96, 7.17 and 7.80 ppm. The peaks of the fluorenyl groups (5, 6, 7 and 8) appear respectively at $\sim d_{\text{H}}$ 7.38, 7.26, 7.42 and 7.77 ppm in the spectrum. These peaks were

consistent with the values found in literature (Watanabe *et al.*, 2003).

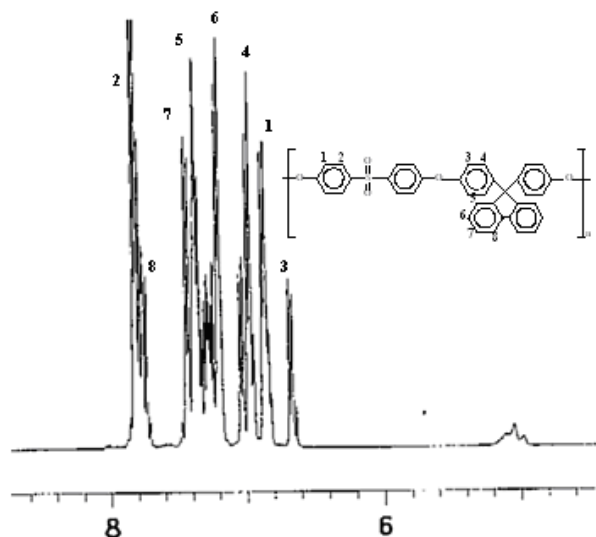
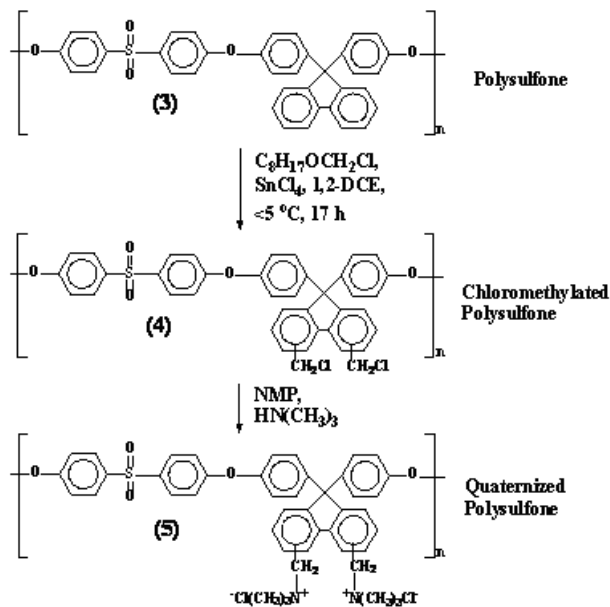


Figure 3: $^1\text{H-NMR}$ spectrum of compound (3)

Chloromethyloctyl ether was synthesized in good yields by bubbling HCl gas through 1-octanol in the presence of paraformaldehyde in DCE (Warszawsky and Dashe, 1985). The conversion of 1-octanol into chloromethyloctyl ether was also verified by $^1\text{H-NMR}$ and FT-IR spectroscopy.

The quaternary ammonium polymers were synthesised in a two-step sequence as depicted, by way of example, in Scheme 2: the reaction of polymer (3) with chloromethyloctyl ether and a Lewis-acid catalyst afforded chloromethylated polysulfone (4), followed by amination with trimethylamine in the presence of NMP to form quaternary polysulfone (5).



Scheme 2: Quaternisation of PAEs

Similarly, compounds (6) and (7), shown below, were synthesised from corresponding PAE base polymers (commercially available) following the same procedure.

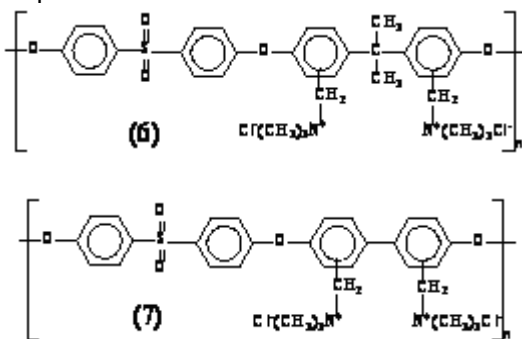


Figure 4 shows $^1\text{H-NMR}$ spectra of the series of chloromethylated polysulfones synthesised in this study. They all showed one main signal for every polymer at ca. 4.50 ppm. This peak indicates the successful incorporation of CH_2Cl groups in the parent polymer. As the quaternised polymers were not soluble in CDCl_3 , no $^1\text{H-NMR}$ spectra were drawn.

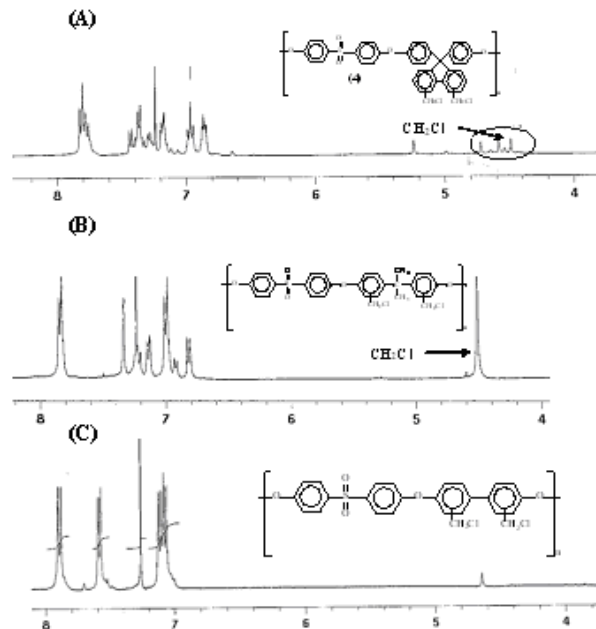


Figure 4: $^1\text{H-NMR}$ spectra of chloromethylated PAEs

The chemical structures of chloromethylated and quaternised polymeric membranes were also confirmed by FT-IR spectroscopy as shown in Figure 5.

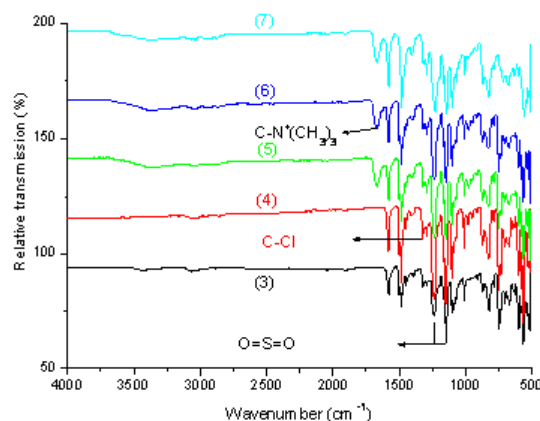


Figure 5: FT-IR spectra of compounds (3) to (7)

The IR absorption bands at 1485 and 1586 cm^{-1} are characteristic of phenyl groups. Comparing compounds (4-7) in Figure 5, shows a new characteristic band of the aminated aromatic salts at 1667 cm^{-1} and the intensity of these characteristic absorption bands increases with the amination content, which confirms the successful

introduction of ammonium groups into the polymer. A peak at 1321 cm^{-1} was also observed, which is attributed to C-Cl groups, indicating that chloromethylation was successful. Characteristic peaks at 1152 and 1240 cm^{-1} were also observed and assigned to O=S=O groups.

The base polymer (3), its chloromethylated analogue (4) and the corresponding quaternised analogue (5) were compared for thermal weight loss behaviour in a nitrogen atmosphere at a heating rate of 10°C per minute by submitting them to a thermogravimetric programme from $0 - 800^\circ\text{C}$ as shown in Figure 6. Stability study of (3) and (4) revealed that these compounds were stable at temperatures of up to ca. 280°C .

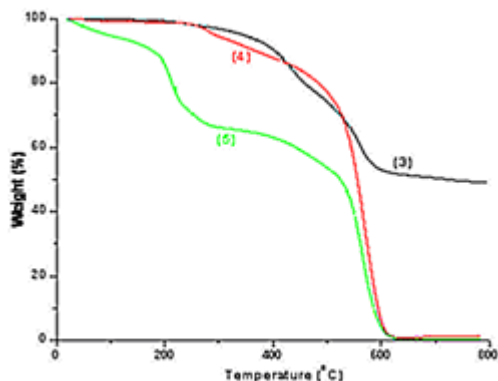


Figure 6: TGA curves of PAEs (3) to (5)

The three quaternised polymers (5, 6, 7) were also analysed thermogravimetrically. Three consecutive weight loss steps were observed, as can be seen in Figure 7:

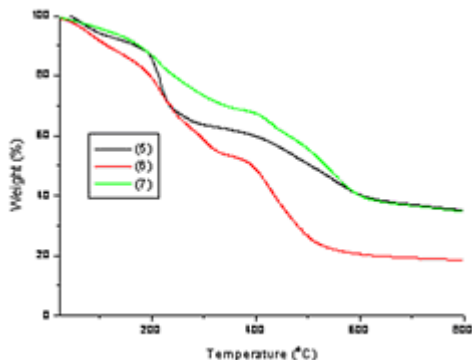


Figure 7: TGA curves of quaternised PAEs

The first weight loss up to 150°C is associated with the loss of absorbed water molecules. The second weight loss at around 220°C is attributed to the loss of quaternary ammonium groups. In the third weight loss region ($T > 420^\circ\text{C}$), the residual polymer backbone is thermally decomposed. Percentages of weight loss for all quaternised polymers at different temperature ranges are summarised in Table 3.

Table 3: Weight loss of quaternised polymers

Polymer	Weight loss (%)	Temperature ($^\circ\text{C}$)
5	29.68	216
	25.17	475
6	35.07	240
	34.75	425
7	28.86	215
	31.97	427

The 5% weight loss temperature range of the membranes is from $215 - 475^\circ\text{C}$. Thermal stability of the quaternised membranes was found to be comparable to that of some other reported PAEs and Nafion membranes (Surowiec and Bogoczek, 1988).

3. Research Outputs

3.1 Test cell

A fuel cell design by the Advanced Energy Systems Group of the Helsinki University of Technology, featuring a double serpentine flow field, was modified for our work.

The design factors considered for addition or modification included:

- Increased active surface area (higher output)
- Ability to upgrade from single cell to stack
- Facility for temperature measurement
- Facility for temperature control

These features were incorporated into a new design, by

- increasing the active surface area from about 18 cm^2 to 24 cm^2 ,
- making the end-plate geometry versatile and sturdy enough to accommodate more than one cell,

- including a channel for a thermocouple in the flow-field plates, and
- including a heating / cooling channel in the end-plates.

4. Conclusions and future work

4.1 Hydrogen fuel cells

The optimum ionomer content was determined as 41% of the Pt/C mass at Pt loadings of 0.05 to 0.15 mg/cm². This correlated well with similar studies in literature. An increase beyond this optimum value did not enhance the performance further.

4.2 Direct alcohol fuel cells

Two types of Pt-Ru/C catalyst were prepared for DMFC, but did not show superior activity (i.e. lower onset potential) to commercially available catalysts. Research in this field is ongoing and may include the use of carbon nanotubes as catalyst support.

A number of mono- and polyhydric alcohols were compared as fuels for a PEM-type DMFC. Isopropanol exhibited the best performance, while ethylene glycol and glycerol showed the weakest performance. Future work will be aimed at explaining these results further and optimising the performance of the poly-ols.

4.3 Anionic membranes

Various ammonium-type anion exchange membranes were synthesised and characterised. They will subsequently be evaluated in terms of methanol permeability as a function of temperature, as well as ionic conductivity as a function of OH⁻ concentration from 25 - 70°C. This investigation will determine the suitability of these membranes for possible subsequent use in direct alcohol alkaline fuel cells.

4.4 Test cell

An existing design for a test cell was improved in terms of active surface area, upgrading to a multi-cell stack, as well as temperature measurement and control. These improvements allow the cell to be used in conjunction with a FuelCon Evaluator C050 test rig in performance tests, in order to control temperature, humidification of reactant

gases, gas flow rates and electric load, thus giving control over a wide range of parameters.

5. References

ACGIH. American Conference of Governmental Industrial Hygienists, Inc. Documentation of the Threshold Limit Values and Biological Exposure Indices, 6th ed., 903-905.

Burstein, G.T., Barnett, C.J., Kucernak, A.R. and Williams, K.R.; *Catal. Today* **38** (1997), 425.

Chen, J., Xu, H., Zhang, H. and Yi, B.; *J. Power Sources* **182** (2008), 531.

Fang, J. and Shen, P.K.; *J. Membr. Sci.* **285** (2006), 317.

Hergenrother, M., Jensen, B.J. and Havens, S.J.; *Polymer* **29** (1988), 358.

Jung, E.H., Jung, U.H., Yang, T.H., Peak, D.H., Jung, D.H. and **Kim, S.H.**; *Int. J. Hydrogen Energy* **32** (2007), 903.

Lee, C.G., Umeda, M. and Uchida, I.; *J. Power Sources* **160** (2006), 78.

Lee, S.J., Mukerjee, S., McBreen, J., Rho, Y.W., Kho, Y.T. and Lee, T.H.; *Electrochim. Acta*, **43** (24) (1998), 3693.

Litster, S. and McLean, G.; *J. Power Sources* 130 (1-2), (2004), 61.

Mauritz, K.A. and Moore, R.B.; *Chem. Rev.* **104** (2004), 4535.

Wang, F., Hickner, M., Kim, Y.S., Zawodzinski, T.A. and **McGrath, J.E.**; *J. Membr. Sci.* **197** (2002), 231.

Matsuoka, K., Iriyama, Y., Abe, T., Matsuoka M. and **Ogumi, Z.**; *J. Power Sources* **150** (2005), 27.

Passalacqua, E., Lufrano, F., Squadrito, G., Patti, A. and Giorgi, L.; *Electrochim. Acta* **43** (24) (1998), 3665.

Passalacqua, E., Lufrano, F., Squadrito, G., Patti, A. and Giorgi, L.; *Electrochim. Acta* **46** (2001), 799.

- Qi, Z. and Kaufman, A.; *J. Power Sources* **111** (2002) 181.
- Reiner, A., Steiger, B., Scherer, G.G. and Wokaun, A.; *J. Power Sources* **156** (2006), 28].
- Savadogo, O.; *J. New Mater. Electrochem. Syst.* **1** (1998), 47.
- Savadogo, O.; *J. Power Sources* **127** (2004), 135.
- Song, J.M., Cha, S.Y. and Lee, W.M.; *J. Power Sources* **94** (2001), 78.
- Surowiec, J. and Bogoczek, R.; *J. Thermal Anal.* **33** (1988), 1097.
- Varcoe, J.R. and Slade, R.C.T.; *Fuel Cells* **5** (2005), 187.
- Warshawsky, A. and Dashe, A.; *J. Polym. Sci.* **23** (1985), 1839.
- Watanabe, M., Uchida, M. and Motoo, S.; *J. Electroanal. Chem.* **229** (1987), 395.
- Watanabe, M.; *Catalysis and electrocatalysis at nanoparticle surfaces*, CRC Press - Taylor and Francis Group (2003), Chapter 22: Design of electrocatalysts for fuel cells, 827.
- Miyatake, K., Chikashige, Y. and **Watanabe, M.**; *Macromolecules* **36** (2003), 9691.
- Wilson, M.S., Valerio, J.A. and Gottesfeld, S.; *Electrochim. Acta* **40** (3), (1995), 355.
- Xue, X., Ge, J., Liu, C., **Xing, W.** and Lu, T.; *Electrochem. Comm.* **8** (2006), 1280.
- Yousfi-Steiner, N., Moçotéguy, Ph., Candusso, D., Hissel, D., Hernandez, A. and Aslanides, A.; *J. Power Sources* **183** (1), (2008), 260.
- Zawodzinski, T.A., Jr., Lopez, C., Jestel, R., Valerio, J and Gottesfeld, S.; *J. Electrochemical Society* **140** (1993), 1981.